Published in final edited form as:
*Neuroscience*. 2010 March 31; 166(3): 796–807. doi:10.1016/j.neuroscience.2010.01.021.

# Alterations in brain antioxidant enzymes and redox proteomic identification of oxidized brain proteins induced by the anti-cancer drug Adriamycin: Implications for oxidative stress-mediated chemobrain

**Gururaj Joshi**[1,2,‡], **Christopher D. Aluise**[1,2,‡], **Marsha Paulette Cole**[4], **Rukhsana Sultana**[1,2], **Mary Vore**[4], **Daret K. St Clair**[4], and **D. Allan Butterfield**[1,2,3,*]

[1] Department of Chemistry, University of Kentucky, Lexington, KY 40506, USA

[2] Center of Membrane Sciences, University of Kentucky, Lexington, KY 40506, USA

[3] Sanders-Brown Center on Aging, University of Kentucky, Lexington, KY 40506, USA

[4] Department of Toxicology, University of Kentucky, Lexington, KY 40506, USA

## Abstract

Adriamycin (ADR) is a chemotherapeutic for the treatment of solid tumors. This quinone-containing anthracycline is well known to produce large amounts of reactive oxygen species (ROS) *in vivo*. A common complaint of patients undergoing long-term treatment with ADR is somnolence, often referred to as "chemobrain." While ADR itself does not cross the blood brain barrier (BBB), we recently showed that ADR administration causes a peripheral increase in tumor necrosis factor α (TNF- α), which migrates across the BBB and leads to inflammation and oxidative stress in brain, most likely contributing to the observed decline in cognition. In the current study, we measured levels of the antioxidant glutathione (GSH) in brains of mice injected intraparitoneally (i.p.) with ADR, as well as the levels and activities of several enzymes involved in brain GSH metabolism. We observed significantly decreased GSH levels, as well as altered GSH/GSSG ratio in brains of ADR treated mice relative to saline- treated controls. Also observed in brains of ADR treated mice were increased levels of glutathione peroxidase (GPx), glutathione-S-transferase (GST), and glutathione reductase (GR). We also observed increased activity of GPx, but a significant reduction in GST and GR activity in mice brain, 72 hrs post i.p injection of ADR (20 mg/kg body weight). Furthermore, we used redox proteomics to identify specific proteins that are oxidized and/or have differential levels in mice brains as a result of a single i.p. injection of ADR. Visinin like protein 1 (VLP1), peptidyl prolyl isomerase 1 (Pin1), and syntaxin 1 (SYNT1) showed differential levels in ADR treated mice relative to saline-treated controls. Triose phosphate isomerase (TPI), enolase, and peroxiredoxin 1 (PRX-1) showed significantly increased specific carbonylation in ADR treated mice brain. These results further support the notion ADR induces oxidative stress in brain despite not crossing the BBB, and that antioxidant intervention may prevent ADR-induced cognitive dysfunction.

*Address for Correspondence and reprint request to: Prof. D. Allan Butterfield, Department of Chemistry, Center of Membrane Sciences, and Sanders-Brown Center on Aging, University of Kentucky, Lexington, KY 40506, USA, Ph: 859-257-3184, FAX: 859-257-5876, dabcns@uky.edu.
‡Both authors contributed equally to this work.

**Keywords**

Adriamycin (doxorubicin); Glutathione; Glutathione-related enzymes; Oxidative stress, chemobrain; proteomics

## Introduction

Free radical-mediated oxidative stress has been implicated in many neurodegenerative disorders (Hensley et al., 1995, Stadtman and Berlett, 1997, Markesbery and Lovell, 1998, Butterfield et al., 2001, Butterfield and Lauderback, 2002). Overproduction of reactive oxygen species (ROS) and reactive nitrogen species (RNS), a decreased antioxidant defense system, or both typically results in significant protein oxidation (Hensley et al., 1995, Stadtman and Berlett, 1997), lipid peroxidation (Markesbery and Lovell, 1998, Butterfield and Lauderback, 2002), and DNA/RNA oxidation (Butterfield et al., 2001).

Adriamycin (ADR) is a quinone-containing chemotherapeutic drug. ADR intercalates into the major grooves of cancerous DNA and inhibits replication and synthesis (Cummings et al., 1991). It is also widely accepted that ADR produces large amounts of ROS in defense against solid tumors (Kappus, 1987, Gutierrez, 2000, Singal et al., 2000); however, this mechanism of action is implicated in the toxicity of several non-targeted organs and limits its dosage in cancer patients. The quinone in ADR undergoes a one-electron reduction to produce a semiquinone, which, in the presence of molecular oxygen, generates superoxide ($O_2^{\bullet -}$) as the semiquinone is recycled to a quinone (a process called redox cycling) (Handa and Sato, 1975, Gutteridge, 1984). Administration of ADR has been documented to cause oxidative stress in non-targeted organs, consistent with the notion that ADR redox cycling results in the generation of significant amounts of ROS (Chen et al., 2007). For instance, free radical mediated protein oxidation and lipid peroxidation have been reported in cardiomyocytes treated with ADR, and ADR-induced ROS production in cardiomyocytes is blocked by antioxidants (DeAtley et al., 1998, DeAtley et al., 1999, Lien et al., 2006).

Apart from cardiomyopathy, patients under long-term treatment with ADR often complain of dizziness, forgetfulness, lack of concentration, and cognitive impairment (somnolence, often called “chemobrain”), sometimes lasting years after cessation of chemotherapy (Meyers, 2000, Schagen et al., 2001, Freeman and Broshek, 2002, Ahles and Saykin, 2007). Recently, we showed that administration of ADR induces a peripheral increase in the cytokine tumor necrosis factor alpha (TNFα), which migrates across the blood brain barrier (BBB) and induces several inflammatory pathways, including glial cell activation (Tangpong et al., 2006, Tangpong et al., 2007, Tangpong et al., 2008). Because ADR itself cannot cross the BBB, the toxic side effects in brain conceivably could be due to TNFα mediated glial activation, resulting in more TNFα production, which can further lead to increased mitochondrial impairment and production of ROS/RNS (Tangpong et al., 2006, Tangpong et al., 2008). This cytokine is strongly implicated in ADR-induced cognitive dysfunction, as mice treated with anti-TNF antibody have no increased brain TNF or mitochondrial dysfunction (Tangpong et al., 2006). Although the biochemical basis for ADR-mediated cognitive dysfunction is not well established, ADR has been shown to cause increased protein oxidation and lipid peroxidation, along with increased MRP-1 expression, in brain isolated from ADR-injected mice (Joshi et al., 2005, Joshi et al., 2007).

Glutathione (GSH) is a major intracellular antioxidant present ubiquitously in the millimolar range throughout the brain. GSH detoxifies intracellular $H_2O_2$ to $H_2O$ and $O_2$ via subsequent oxidation to glutathione disulfide (GSSG) by the enzyme glutathione peroxidase (GPx). GSSG is recycled to GSH via glutathione reductase (GR). The GSH/GSSG ratio is critical to

maintaining the intracellular redox balance (Smith et al., 1996). GSH is also capable of conjugating to αβ-unsaturated aldehydes, which are products of lipid peroxidation, by the cytosolic enzyme glutathione-S-transferase (GST). GST-mediated glutathione-S conjugates are exported from the cell via multi drug resistant protein-1 (MRP-1), an ATP-binding cassette (ABC) transporter (Nies et al., 2004, Sultana and Butterfield, 2004). Depletion of GSH in specific brain regions and/or the concomitant increase in GSSG levels contribute to the oxidative stress-mediated neuronal dysfunction in various neurodegenerative disorders (Benzi and Moretti, 1995, Butterfield and Sultana, 2007). Also contributing to the oxidative stress observed in these disorders is altered activities or levels of enzymes involved in GSH metabolism, namely GPx, GR, and GST. Given that oxidative stress and mitochondrial dysfunction occur in brain following intraparitoneal (i.p.) administration of ADR, we tested the hypothesis that in vivo ADR modulates the GSH antioxidant defense system in brain.

Redox proteomics has been used to identify proteins with differential levels and adverse protein modifications in disease conditions to shed light on a specific pathology (Butterfield and Sultana, 2007). To date, two studies have shown globally increased levels of protein carbonyls in brains of mice treated i.p. with ADR compared to controls (Joshi et al., 2005, Joshi et al., 2007). Using redox proteomics, it is possible to separate proteins in two dimensions in order to detect which specific proteins experience an increase in carbonylation (or other modification) as a result of an oxidative insult. Therefore, in addition to isolating specific antioxidant proteins for analyses of levels and activity, a second goal of this study was to use redox proteomics to identify proteins in brains of ADR treated mice with differing levels and/or increases in specific oxidation as a result of a single i.p injection of this chemotherapeutic agent. The results shown here are discussed with relevance to chemobrain following ADR-induced free radical-mediated oxidative stress.

## Materials and Methods

### Animals

Male B6C3 mice (2–3 months of age), approximately 30 g in size, housed in the University of Kentucky Central Animal Facility in 12 h light/dark conditions and fed standard Purina rodent laboratory chow ad libitum, were used. The animal protocols were approved by the University of Kentucky Animal Care and Use Committee.

### Chemicals

Doxorubicin HCl (ADR) was purchased from Bedford Laboratories™. All other chemicals were purchased from Sigma-Aldrich (St. Louis, MO), unless stated otherwise. The primary antibodies for GST and GPx were purchased from Chemicon International (Temecula, CA). The primary antibody for GR was purchased from Abcam, Inc (Cambridge, MA). Criterion PreCast Tris-HCl polyacrylamide gels (12.5%) and Trans-Blot Transfer Medium nitrocellulose membranes (0.45 μm) were purchased from BioRad (Hercules, CA). The GSH assay kit was purchased from Cayman Chemicals (Ann Arbor, MI).

### Preparation of brain homogenate

Brains were isolated and dissected following sacrifice by decapitation from mice injected intraperitoneally (i.p.) with ADR (20 mg/kg body weight), 72 h post i.p. injection, or from saline-treated control mice. The ADR dosage and time were based on prior studies (Joshi et al., 2005). Isolated brains were homogenized in ice cold lysing buffer containing 4 μg/ml leupeptin, 4 μg/ml pepstatin, 5 μg/ml aprotinin, 2 mM ethylenediaminetetraacetic acid (EDTA), 2 mM ethylene glycol-bistetraacetic acid (EGTA) and 10 mM 4-(2-hydroxyethyl)-1-piperazine-ethanesulfonic acid (HEPES), pH 7.4, at a ratio of 10% w/v. Each brain was homogenized by 20 passes of a Wheaton tissue homogenizer, and the resulting homogenate

was centrifuged at 1500g for 10 mins. The pellet (nuclear fraction) was suspended in 1ml phosphate buffered saline (PBS) containing 0.01% (w/v) sodium azide and 0.2% (v/v) Tween 20. The supernatant was retained and centrifuged at 20000 g for 10 mins. The pellet (membrane fraction) was suspended in 1ml PBS and the supernatant (cytosolic fraction) was retained for GSH measurement and enzyme activities. All the fractions suspended in PBS were washed twice with PBS at 32000 g for 10 min. The resulting fractions were assayed for protein concentration by the Pierce BCA method.

## GSH/GSSG assays

GSH and GSSG were measured using the method of Hissin and Hilf. The supernatant obtained from homogenate was deproteinated with 10% meta phosphoric acid and the deproteinated supernatant was used for GSH/GSSG assays. GSH was measured by adding sample (10 μl) to 10 μl of o-phthalaldehyde (1 mg/mL in reagent grade methanol) and 0.1 M phosphate-buffered saline (pH 8) with 5 mM EDTA, and measured fluorometrically (λex= 350nm, λem= 420nm). GSSG was measured by adding 10 μl of deproteinated sample to 0.04 M N-ethylmaleimide, o-phthaladehyde, and 0.1 N NaOH, and measured fluorometrically (λex= 350nm, λem= 420nm) (Hissin and Hilf, 1976).

## Western blots

Samples (100 μg) were incubated with sample loading buffer and were denatured and electrophoresed on a 12.5% SDS-polyacrylamide gel. Proteins were transferred to a nitrocellulose membrane at 90 mA/gel for 2 h. The blots were blocked for 1h in fresh wash buffer (10 mM Tris-HCl, pH7.5), 150 mM NaCl, 0.05% Tween 20, pH 7.4, containing 3% bovine serum albumin) and incubated with a 1:1000 dilution of the respective anti- GST, GPx or GR monoclonal antibody in phosphate buffered saline containing 0.01% (w/v) sodium azide and 0.2% (v/v) Tween 20 (PBS) for 1 h. Membranes were washed three times in PBS and incubated for 1 h with anti-rabbit IgG alkaline phosphatase secondary antibody diluted in PBS in a 1:8000 ratio. Membranes were washed three times in PBS for 5 min and developed using SigmaFast tablets (BCIP/NBT substrate).

In all cases non-specific background labeling by secondary antibody was negligible.

## Enzyme activity assays

**Estimation of glutathione-S-transferase activity—**GST (EC 2.5.1.18) activity was measured using a reaction mixture consisting of 0.1 M phosphate buffer (pH 6.5), 1.0 mM reduced glutathione, 1.0 mM CDNB and 1 mg/ml of supernatant protein (Habig et al., 1974). The changes in absorbance were recorded at 340 nm in a 96 well microtiter plate, and the enzymatic activity was calculated as nmol of CDNB conjugate formed $min^{-1}$ $mg^{-1}$ protein.

**Estimation of glutathione peroxidase activity—**GPx (EC 1.11.1.9) was measured using a reaction mixture consisting of 0.2 mM $H_2O_2$, 1.0 mM GSH, 0.14 U of glutathione reductase GR, 1.5 mM NADPH, 1.0 mM sodium azide, 0.1 M phosphate buffer (pH 7.4) and 1 mg/ml of supernatant protein (Wheeler et al., 1990). The changes in absorbance were recorded at 340 nm in a 96 well microtiter plate and enzyme activity was calculated as nmol of NADPH oxidized $min^{-1}$ $mg^{-1}$ protein.

**Estimation of glutathione reductase activity—**The GR (EC 1.6.4.2) activity assay reaction mixture consisted of 0.1 M phosphate buffer (pH 7.6), 0.5 mM EDTA, 1.0 mM oxidized glutathione, 0.1 mM NADPH and 1 mg/ml of supernatant protein in a total volume of 200 μl (Carlberg and Mannervik, 1985). The enzyme activity was assayed in a 96-well plate reader by measuring the disappearance of NADPH at 340 nm and was calculated as nmol of NADPH oxidized $min^{-1}$ $mg^{-1}$ protein.

## Redox Proteomics

**Sample Preparation—**To derivatize protein carbonyl groups, 150 μg of brain homogenate was incubated with 4 volumes of 2,4-dinitrophenylhydrazine (DNPH; 20 mM in 2 M HCl) or 2 N HCl (for 2-D gel protein mapping and mass spectrometry analysis) at room temperature for 30 min and then mixed with ice-cold trichloroacetic acid (final concentration,15%) and incubated on ice for 10 min. Precipitates were centrifuged at 14,000 g at 4°C for 2 min. The pellets were washed with 500 μl of ethyl acetate/ethanol (1/1, v/v) three times. The final pellet was dissolved in 200 μl of rehydration buffer containing 7 M urea, 2 M thiourea, 2% Chaps, 0.8% (v/v) Ampholyte, pH 3–10, 1% zwittergent, 45 mM DTT, and a trace amount of bromophenol blue. Samples were then sonicated on ice for 20 s three times.

**Two-dimensional gel electrophoresis—**IPG strips were actively rehydrated with 200 μl of samples at 50 V and 20°C for 16 h. Isoelectric focusing (IEF) was performed at 20°C in a Protean IEF cell (Bio-Rad) as follows: 800 V for 2 h linear gradient, 1200 V for 4 h slow gradient, 8000 V for 8 h linear gradient, and 8000 V for 10 h rapid gradient. After IEF, the strips were stored at −80°C until processing. Before the second-dimension separation, the strips were equilibrated in 0.375 M Tris–HCl (pH 8.8) containing 6 M urea, 2% sodium dodecyl sulfate, 20% (v/v) glycerol, and 0.5% DTT for 10 min, followed by a reequilibration in a similar buffer containing 4.5% iodoacetamide in place of DTT for 10 min. Strips were placed on the Criterion precast gels and electrophoresed at 200 V for 65 min. Gels of HCl-treated samples were fixed in a solution containing 10% (v/v) methanol, 7% (v/v) acetic acid for 30 min and stained in SYPRO Ruby gel stain (50 ml/gel) with agitation at room temperature overnight. The gels were rinsed in the fixing solution for 60 min to remove background stain and washed with deionized water. Images of the stained gels were obtained using a fluorescence imager, Storm 860 ($\lambda_{ex}$ = 470 nm, $\lambda_{em}$ = 618 nm; Molecular Dynamics, Sunnyvale, CA, USA).

**Two-dimensional oxyblot—**Gels of DNPH treated samples were transferred to a nitrocellulose membrane at 90 mA/gel for 2 h and blocked for 2 h with 3% bovine serum albumin (BSA) in PBS. Blots were incubated with primary rabbit anti-DNP antibody (1:200) for 2 h. Membranes were washed three times in PBS and incubated for 1 h with an anti-rabbit IgG alkaline phosphatase secondary antibody diluted in PBS in a 1:8000 ratio. The membrane was washed three times in PBS for 5 min and developed using SigmaFast tablets (BCIP/NBT substrate).

**Image analysis—**PDQuest software (Bio-Rad) was used to analyze the gels and the blots and to compare protein and carbonyl contents in brain samples of saline- and ADR-treated mice. Densitometric intensity of Sypro Ruby stained gels corresponded to protein levels on 2D gels; specific carbonyl content was assessed by the spot intensity on 2D Western blots divided by the corresponding protein level as assessed by 2D gel quantitation. Spot intensities were normalized relative to total density of spots in corresponding gel or blot to correct for slight differences in staining and/or loading.

## In-gel digestion

Only spots found to be statistically significantly different for protein levels or specific carbonylation compared to control were subject to in gel digestion. Samples were prepared according to the method described by Thongboonkerd et al. (Thongboonkerd et al., 2002). Briefly, the gel piece containing the protein of interest was cut out from the gel with a clean razor blade and transferred into a 1.5-ml microcentrifuge tube. The gel piece was incubated with 30 μl of 0.1 M $NH_4HCO_3$ at room temperature for 15 min, then for another 15 min after the addition of 30 μl of acetonitrile, and was air-dried for 30 min after the removal of the liquid. The gel piece was rehydrated with 20 μl of 20 mM DTT in 0.1 M $NH_4HCO_3$ at 56°C for 45 min. Next, the gel piece was incubated with 20 μl of 55 mM iodoacetamide in 0.1 M

$NH_4HCO_3$ in the dark at room temperature for 30 min. Gel plug was incubated with 30 μl of 50 mM $NH_4HCO_3$ at room temperature for 15 min, then for another 15 min after the addition of 30 μl of acetonitrile, and was air dried for 30 min after the removal of the liquid. The gel piece was rehydrated with the addition of a minimal volume of 20 ng/μl modified trypsin in 50 mM $NH_4HCO_3$ and was incubated with shaking at 37°C overnight (18 h).

### Mass spectrometry and protein identification

Peptides resulting from in-gel trypsin digestion were spotted on a 384-position, 600-μm AnchorChip Target (Bruker Daltonics, Bremen, Germany) and prepared according to AnchorChip recommendations (AnchorChip Technology, Rev. 2; Bruker Daltonics). Briefly, 1 μl of sample was mixed with 1 μl of α-cyano-4-hydoxycinnamic acid (0.3 mg/ml in ethanol:acetone, 2:1) directly on the target and dried at room temperature. The sample spot was washed with 1 μl of a 1% trifluoroacetic acid (TFA) solution for approximately 60 s. The TFA droplet was gently blown off the sample spot with compressed air. The resulting diffuse sample spot was recrystallized (refocused) using 1 μl of a solution of ethanol:acetone:0.1% TFA (6:3:1). Spectra were recorded on a Spec 2E matrix-assisted laser desorption ionization–time of flight mass spectrometer in the reflectron mode as summations of 100 laser shots. External calibration of the mass axis was used for acquisition, and internal calibration using either trypsin autolysis ions or matrix clusters was applied postacquisition for accurate mass determination. Peptide mass fingerprinting was used to identify proteins from tryptic peptide fragments by utilizing the MASCOT search engine (http://www.matrixscience.com) based on the entire SwissProt protein database. Database searches were conducted allowing for up to one missed trypsin cleavage and using the assumption that the peptides were monoisotopic, oxidized at methionine residues, and carbamidomethylated at cysteine residues. Mass tolerance of 100 ppm was the window of error allowed for matching the peptide mass values. Probability-based MOWSE scores were estimated by comparison of search results against estimated random match population and were reported as $-10 \times \log_{10}(P)$, where P is the probability that the identification of the protein is not correct. MOWSE scores greater than 54 were considered to be significant ($p < 0.05$). All proteins identified were within the expected size and pI range based on the positions in the gel.

**Statistical analysis—**A two-tailed Student's t-test was used to assess statistical significance. P values <0.05 were considered significant for comparison between control and experimental data sets.

## Results

### Brain GSH/GSSG assay

GSH levels in a system are closely regulated and are indicative of its cellular redox balance. A reduction in GSH or the GSH/GSSG ratio may be an indication of redox imbalance or oxidative stress (Watson et al., 2003). Figure 1a shows a significantly lower GSH level in brain isolated from ADR-injected mice compared to saline-injected controls ($p < 0.001$). Also, we observed a significant decrease in the GSH/GSSG ratio in ADR treated mice relative to controls (Fig 1b).

### Expression levels of GPx, GST, and GR in brain isolated from ADR treated mice and saline-treated controls

Figure 2a shows the Western blots of GST, GPx and GR in brain isolated from mice injected i.p. with saline or ADR. GAPDH was used as a loading control. Normalized enzyme levels corresponding to western blots in Figure 2a are shown in Figures 2b, 2c, and 2d. As evident from the figures, there is a significant increase in the expression of GST, GPx and GR in brain isolated from ADR-injected mice when compared to saline-injected controls ($p < 0.05$).

### Enzyme activities of GPx, GST, and GR in brain isolated from ADR treated mice and saline-treated controls

Table I shows the activity of GSH-related enzymes GST, GPx and GR, in brain isolated from saline and ADR injected mice, respectively. There was a significant increase in the activity of GPx, while significantly reduced activities of GST and GR were observed in brain isolated from ADR-injected mice compared to saline-injected controls ($p < 0.05$).

### Redox proteomics analysis to identify oxidized and differential levels of brain proteins following ADR treatment

Proteomics and redox proteomics have been used, respectively, to identify differential levels and oxidative modifications of brain proteins in neurodegenerative diseases such as Alzheimer's disease (AD) and mild cognitive impairment (MCI) (Butterfield and Sultana, 2007). Figure 3 shows representative 2D gels of brains from mice treated i.p. with saline and ADR, respectively. After analysis, three proteins in brain showed significantly decreased levels in ADR treated mice relative to saline-treated controls. These proteins that were identified by mass spectrometry and subsequent interrogation of protein databases were syntaxin 1 (SYNT1), visinin like protein 1 (VLP1), and peptidyl prolyl isomerase A (Pin1) (Figures 3, 4). Fig 3 displays geographical location of these proteins with respect to isoelectric point and molecular weight on 2D gel maps from saline and ADR treated mice brains. Fig. 4 shows expansions of gel images to show more clearly the loss of proteins in brain following i.p. ADR treatment. Table II displays the proteins identified by proteomics as having altered levels in brains of ADR treated mice relative to saline-treated controls; the implications of these protein changes in brain with respect to cognitive impairment are discussed below.

Oxidative stress leads to significant protein oxidation (Stadtman and Berlett, 1997). Protein oxidation leads to a conformational change in tertiary structure, which typically results in altered activity (Stadtman and Berlett, 1997, Butterfield et al., 2006b). Densitometric analysis of 2D western blots and gels revealed 3 spots that corresponded to significantly increased oxidation in brain isolated from ADR-treated mice relative to control. These protein spots were identified as triose phosphate isomerase (TPI), alpha-enolase, and peroxiredoxin 1 (PRX-1) (Figure 5). Fig 3 displays the respective locations of these proteins on 2D gel maps of control and ADR treated mice brains. Figs 5a & 5b are magnified images of gels and oxyblots clearly illustrating increases in specific oxidation of proteins reported in Table 3. A summary of the protein identifications that were found to be increasingly carbonylated in brains of ADR treated mice is displayed in Table III. The implications of the oxidation of these brain proteins with respect to cognitive decline are discussed below.

## Discussion

A decrease in total GSH levels, or an imbalance in the ratio of reduced to oxidized GSH may index and/or cause oxidative stress that leads to protein oxidation (Stadtman and Berlett, 1997), lipid peroxidation (Markesbery and Lovell, 1998), and DNA/RNA oxidation (Butterfield et al., 2001). GSH is known to protect against cellular free radical-mediated oxidative damage by functioning as an oxyradical scavenger, thereby reducing lipid peroxidation (Meister and Anderson, 1983, Darley-Usmar and Halliwell, 1996, Sies, 1999, Schulz et al., 2000). GSH, apart from its endogenous antioxidant activity, also has roles in a wide range of metabolic processes, such as activation of transcription factors, DNA repair, regulation of enzyme activity, and biosynthetic processes (Meister, 1995).

The nervous system is particularly susceptible to oxidative insults because of high levels of polyunsaturated fatty acids, high oxygen consumption, and low antioxidant capacity. Hence, the brain is heavily dependent on GSH as a primary endogenous neuroprotectant. GSH

detoxifies neurons from HNE and other reactive alkenals and protects brain cells from peroxynitrite-mediated damage (Mark et al., 1997, Koppal et al., 1999). HNE, acrolein, and other lipid peroxidation products are known to damage proteins and other biomolecules in AD brain (Sayre et al., 1997, Markesbery and Lovell, 1998, Butterfield et al., 2006c, Reed et al., 2008a, Perluigi et al., 2009, Reed et al., 2009). These alkenals form an immediate substrate for GSH; consequently, GSH depletion may lead to apoptosis initiated by lipid peroxidation products (Mark et al., 1997, Cenini et al., 2008). In the current study, reduced levels of brain GSH and GSH/GSSG ratios were found in ADR-injected mice when compared to saline-injected controls (Fig. 1). We previously reported increased levels of protein carbonyls, HNE, and 3-nitrotyrosine (3NT) in brain isolated from ADR-injected mice (Joshi et al., 2007). We hypothesize that a reduced level of GSH and/or an imbalance in the GSH/GSSG ratio renders cellular materials vulnerable to oxidative attack, hence contributing to the observed protein oxidation and increased reactive alkenals found in brains of ADR-injected mice. Consistent with the implication of lowered GSH in chemobrain, Konat et al. observed behavioral deficits in rats upon administration of ADR that were alleviated with co-administration of N-acetlycysteine (NAC), a GSH precursor (Konat et al., 2008).

GPx, GR, and GST provide protection to neurons from oxidative stress at the expense of GSH. GPx converts $H_2O_2$ to $H_2O$ and $O_2$. The reducing electrons are provided by GSH as it is converted to GSH disulfide, GSSG. GR converts GSSG back to GSH, utilizing NADPH as a cofactor. GST plays a role in neuroprotection by catalyzing the conjugation of GSH to reactive alkenals, oftentimes products of lipid peroxidation, which are then cleared from neurons by the action of MRP-1 (Sultana and Butterfield, 2004). We previously reported increased levels of brain MRP-1 in ADR-injected mice (Joshi et al., 2005). In the present study, we found significantly increased levels of GST, GPx, and GR (Fig. 2) in brains of mice treated i.p. with ADR. Interestingly, we also found that the activities of GST and GR in brain isolated from ADR-injected mice are significantly decreased compared to saline-treated controls, whereas GPx activity is elevated in brains of ADR treated mice (Table I). Adb El-Gawad et al. (2004) also observed increased activity of GPx in brain isolated from ADR treated mice. An increased activity of GPx and/or a reduced activity of GR could potentially result in increased GSSG levels, thereby altering the GSH/GSSG ratio towards the more oxidized form, leading to oxidative stress, as we observed here. In this study, we find both scenarios occur in brain with i.p. administration of ADR. A reduced GST activity would lead to less clearance of toxic cytosolic alkenals, which may contribute to the observed increase in protein-bound HNE levels in brain from ADR-injected mice. However, the increased expression levels of GST and GR in ADR treated mice brain may be indicative of a cellular stress response to oxidative stress and decreased activity of these enzymes upon administration of ADR, possibly due to oxidative or nitrosative damage (Calabrese et al., 2004). Despite augmented levels of these neuroprotective enzymes to combat diminished activities, oxidative stress is detected in brains of ADR treated mice, implying that these defense mechanisms are incapable of providing protection from ADR induced ROS. We posit that similar changes may occur in brains of patients with chemobrain.

Based on the results presented in this paper and others that suggest the brain undergoes oxidative stress in the form of increased protein carbonylation upon i.p administration of ADR (Joshi et al., 2005, Joshi et al., 2007), the present study also sought to identify specifically carbonylated brain proteins, as well as differentially expressed proteins, in the brains of ADR-injected mice. Using the proteomics approach previously utilized in our laboratory (Castegna et al., 2002, Castegna et al., 2003, Boyd-Kimball et al., 2005, Poon et al., 2005, Boyd-Kimball et al., 2006, Poon et al., 2006, Butterfield and Sultana, 2007, Reed et al., 2008a, Reed et al., 2009), densitometric analysis revealed decreased levels of SYNT1, Pin1, and VLP1 in the brains isolated from ADR- injected mice relative to saline injected controls (Fig. 3 and Table 2). Further, our group showed that the total level of protein carbonyls, a marker of oxidative

damage to proteins, is increased in the brains isolated from ADR-injected mice when compared to saline-injected controls (Joshi et al., 2005, Joshi et al., 2007). In this study, we demonstrate that the specific carbonyl levels of TPI, alpha-enolase, and PRX-1 are significantly increased in brain upon i.p. ADR treatment compared to those in brain from saline-treated controls (Fig. 5a & b and Table 3). Consistent with the notion that chemobrain is associated with ADR-induced alterations in brain proteins, these processes are known to affect cognitive function.

Pin1 is a peptidyl prolyl cis-trans isomerase that catalyzes the cis-trans isomerization of phosphorylated Ser/Thr-Pro protein motifs of target proteins. Isomerization by Pin1 modulates target protein folding, biological activity and stability, and regulation of cell cycle (Lu et al., 1996, Zhou et al., 1999, Winkler et al., 2000, Takahashi et al., 2008). Pin1 is heavily implicated in the pathogenesis of AD, as the dysfunction/downregulation of this protein may be critical to tangle formation, cell loss, and amyloid beta-peptide disruption (Butterfield et al., 2006a). Two papers on Alzheimer's disease from our laboratory show oxidized and/or decreased levels of Pin1 in AD brains relative to non-demented controls (Butterfield et al., 2006b, Sultana et al., 2006a). Our current report on differential levels of brain proteins in ADR treated mice also shows a decreased level of this protein (Fig. 4), consistent with concept that Pin1 may contribute to the disrupted cognition as a result of ADR. Although the nature of this decrease is somewhat unclear as it relates to ADR-induced cognition changes, cancer survivors are more likely to develop cognitive impairment/dementia later in life (Heflin et al., 2005). We speculate that changes in the levels of Pin1 as a result of ADR therapy may accelerate AD pathogenesis years before onset of dementia.

Enolase and TPI are glycolytic enzymes. TPI catalyzes the reversible interconversion of dihydroxyacetone phosphate and glyceraldehyde 3-phosphate, while enolase converts 2-phosphoglycerate to phosphoenolpyruvate. Decreased neuronal ATP production followed by progressive neuronal death has been observed upon inhibition of TPI (Sheline and Choi, 1998). Oxidation of enolase has lead to observed decreases in enzyme activity (Reed et al., 2009). Enolase also has other important functions, including membrane binding and alteration of plasminogen (Allan Butterfield and Bader Lange, 2009). Previous studies from our laboratory have reported oxidation/nitration of TPI and enolase in brain in various stages of AD (Castegna et al., 2003, Butterfield et al., 2006b, Sultana et al., 2006b, Sultana et al., 2006c, Sultana et al., 2007, Reed et al., 2008a, Reed et al., 2008b, Reed et al., 2009). In the current study, we observed an increased carbonylation of TPI and enolase in brain isolated from ADR-injected mice when compared to brain isolated from saline-injected control (Figs 5a & b). Oxidation of TPI after ADR administration also has been observed in heart (Chen et al., 2006). Increased oxidation of these glycolytic enzymes may ultimately result in neuronal death as a result of decreased ATP production, culminating in cognitive deficits observed in chemobrain.

PRX-1 is an antioxidant protein that contains essential catalytic cysteine residues (Yim et al., 1994, Neumann et al., 2003). PRX-1 is ubiquitously expressed predominantly in the cytosol and alternatively in nucleus. In brain, PRX-1 is localized to astrocytes, whereas PRX-2 is expressed in neurons (Sarafian et al., 1999). Transfection studies show that PRX-1 can regulate ROS induced by growth factor signaling and can eliminate peroxides in vivo (Kang et al., 1998). Altered expression of various peroxiredoxins has been observed in oxidative stress-mediated neurodegenerative disorders including AD (Krapfenbauer et al., 2003). In the current study, we observed an increased carbonylation of PRX-1 in brain isolated from ADR-injected mice (Fig 5a). Increased oxidative modification of the antioxidant protein PRX-1 likely would decrease the clearance of various peroxides and increase cytosolic ROS. The primary function of PRX-1 is to scavenge peroxides at the expense of thioredoxin, which, in turn, is modulated by GSH. This result potentially couples oxidation of PRX-1 to loss of GSH noted above. This alteration may be related to the observed ADR-mediated protein oxidation/nitration, lipid

peroxidation, and altered GSH defense in brain as well as cognitive dysfunction in ADR-treated patients.

VLP1 is primarily localized in the plasma membrane, and is predominantly expressed in brain (Bernstein et al., 1999). VLP1 belongs to a family of neuronal $Ca^{2+}$ sensor/binding proteins. Upon binding to $Ca^{2+}$, VLP1 undergoes a conformational change that facilitates its association with lipid bilayers (Ames et al., 1997). VLP1 has also been shown to modulate cGMP signaling pathways in transfected neurons in vitro (Braunewell et al., 2001). VLP1 showed reduced immunoreactivity in neurons from temporal cortex of AD patients (Schnurra et al., 2001). VLP1 may be involved in processes leading to phosphorylation of tau, which, if excessive, can lead to disruption of microtubules with consequent altered anterograde and retrograde transport. Such a scenario would be clearly relevant in conditions in which memory and cognitive functions were compromised. In the current study, we observed a decreased expression of VLP1 in brain isolated from ADR-injected mice compared to brain isolated from saline-injected mice (Fig 4). Lower expression may cause $Ca^{2+}$ dyshomeostasis that conceivably may lead to neuronal apoptosis with subsequent effects on cognition.

SYNT1B2 is an integral membrane transport protein. In neurons, this protein forms an integral part of synaptic vesicles. The primary function of SYNT1B2 is docking/priming of synaptic vesicles at presynaptic active zones (Morciano et al., 2005). Although not widely researched, the expression of syntaxin is known to be decreased in neurons of transgenic mice with altered glial fibrillary acidic protein (GFAP), a model of Alexander's disease, a fatal neurodegenerative disorder resulting from missense mutations of the intermediate filament protein, GFAP (Hagemann et al., 2005). In addition, GFAP is a marker for activated microglia, which could be related to inflammation in brain following ADR. In the present study we observed a decreased level of this protein in brain isolated from ADR-injected mice (Fig 4). Lower expression may result in defective vesicle docking to the presynaptic membrane, which we posit leads to dysfunctional neurotransmitter release, which could be related to cognitive dysfunction associated with chemobrain.

The present data detailing altered GSH-related enzyme activities and identification of differential levels and specifically oxidized brain proteins after a single i.p. injection of ADR are consistent with our previous results in vivo (Joshi et al., 2005, Tangpong et al., 2006, Joshi et al., 2007, Tangpong et al., 2007). ADR-induced oxidative stress, altered GSH metabolism and levels and activity of its related enzymes, TNF-α production, brain mitochondrial dysfunction, and appearance of apoptotic bodies in brain may be related to the observed altered levels or specific oxidation of key proteins contributing to cognitive decline. Therefore, following demonstration that chemotherapeutic outcomes are not compromised, co-administration of antioxidants capable of maintaining the GSH defense system in brain (such as NAC) along with ADR may protect cancer patients from the apparent cognitive rigors of ADR chemotherapy. However, as noted, an important point to emphasize is that any measure taken to reduce harmful side effects of this chemotherapeutic drug must not interfere with the therapeutic efficacy of the drug itself. Studies to further elucidate the neuropathology of ADR induced cognitive dysfunction are underway in our laboratory.

## Acknowledgments

This work was supported in parts by funds from the Markey Cancer Center of the University of Kentucky and NIH grants to DSC [AG-05119; CA-80152; CA-94853].

## References

Ahles TA, Saykin AJ. Candidate mechanisms for chemotherapy-induced cognitive changes. Nature reviews 2007;7:192–201.

Allan Butterfield D, Bader Lange ML. Multifunctional Roles of Enolase in Alzheimer Disease Brain: Beyond Altered Glucose Metabolism. Journal of neurochemistry. 2009

Ames JB, Ishima R, Tanaka T, Gordon JI, Stryer L, Ikura M. Molecular mechanics of calcium-myristoyl switches. Nature 1997;389:198–202. [PubMed: 9296500]

Benzi G, Moretti A. Age- and peroxidative stress-related modifications of the cerebral enzymatic activities linked to mitochondria and the glutathione system. Free radical biology & medicine 1995;19:77–101. [PubMed: 7635361]

Bernstein HG, Baumann B, Danos P, Diekmann S, Bogerts B, Gundelfinger ED, Braunewell KH. Regional and cellular distribution of neural visinin-like protein immunoreactivities (VILIP-1 and VILIP-3) in human brain. Journal of neurocytology 1999;28:655–662. [PubMed: 10851344]

Boyd-Kimball D, Castegna A, Sultana R, Poon HF, Petroze R, Lynn BC, Klein JB, Butterfield DA. Proteomic identification of proteins oxidized by Abeta(1–42) in synaptosomes: implications for Alzheimer's disease. Brain research 2005;1044:206–215. [PubMed: 15885219]

Boyd-Kimball D, Poon HF, Lynn BC, Cai J, Pierce WM Jr, Klein JB, Ferguson J, Link CD, Butterfield DA. Proteomic identification of proteins specifically oxidized in Caenorhabditis elegans expressing human Abeta(1–42): implications for Alzheimer's disease. Neurobiology of aging 2006;27:1239–1249. [PubMed: 16099075]

Braunewell KH, Brackmann M, Schaupp M, Spilker C, Anand R, Gundelfinger ED. Intracellular neuronal calcium sensor (NCS) protein VILIP-1 modulates cGMP signalling pathways in transfected neural cells and cerebellar granule neurones. Journal of neurochemistry 2001;78:1277–1286. [PubMed: 11579136]

Butterfield DA, Abdul HM, Opii W, Newman SF, Joshi G, Ansari MA, Sultana R. Pin1 in Alzheimer's disease. Journal of neurochemistry 2006a;98:1697–1706. [PubMed: 16945100]

Butterfield DA, Drake J, Pocernich C, Castegna A. Evidence of oxidative damage in Alzheimer's disease brain: central role for amyloid beta-peptide. Trends Mol Med 2001;7:548–554. [PubMed: 11733217]

Butterfield DA, Lauderback CM. Lipid peroxidation and protein oxidation in Alzheimer's disease brain: potential causes and consequences involving amyloid beta-peptide-associated free radical oxidative stress. Free radical biology & medicine 2002;32:1050–1060. [PubMed: 12031889]

Butterfield DA, Poon HF, St Clair D, Keller JN, Pierce WM, Klein JB, Markesbery WR. Redox proteomics identification of oxidatively modified hippocampal proteins in mild cognitive impairment: insights into the development of Alzheimer's disease. Neurobiology of disease 2006b;22:223–232. [PubMed: 16466929]

Butterfield DA, Reed T, Perluigi M, De Marco C, Coccia R, Cini C, Sultana R. Elevated protein-bound levels of the lipid peroxidation product, 4-hydroxy-2-nonenal, in brain from persons with mild cognitive impairment. Neuroscience letters 2006c;397:170–173. [PubMed: 16413966]

Butterfield DA, Sultana R. Redox proteomics identification of oxidatively modified brain proteins in Alzheimer's disease and mild cognitive impairment: insights into the progression of this dementing disorder. J Alzheimers Dis 2007;12:61–72. [PubMed: 17851195]

Calabrese V, Boyd-Kimball D, Scapagnini G, Butterfield DA. Nitric oxide and cellular stress response in brain aging and neurodegenerative disorders: the role of vitagenes. In vivo (Athens, Greece) 2004;18:245–267.

Carlberg I, Mannervik B. Glutathione reductase. Methods Enzymol 1985;113:484–490. [PubMed: 3003504]

Castegna A, Aksenov M, Thongboonkerd V, Klein JB, Pierce WM, Booze R, Markesbery WR, Butterfield DA. Proteomic identification of oxidatively modified proteins in Alzheimer's disease brain. Part II: dihydropyrimidinase-related protein 2, alpha-enolase and heat shock cognate 71. Journal of neurochemistry 2002;82:1524–1532. [PubMed: 12354300]

Castegna A, Thongboonkerd V, Klein JB, Lynn B, Markesbery WR, Butterfield DA. Proteomic identification of nitrated proteins in Alzheimer's disease brain. Journal of neurochemistry 2003;85:1394–1401. [PubMed: 12787059]

Cenini G, Sultana R, Memo M, Butterfield DA. Effects of oxidative and nitrosative stress in brain on p53 proapoptotic protein in amnestic mild cognitive impairment and Alzheimer disease. Free radical biology & medicine 2008;45:81–85. [PubMed: 18439434]

Chen Y, Jungsuwadee P, Vore M, Butterfield DA, St Clair DK. Collateral damage in cancer chemotherapy: oxidative stress in nontargeted tissues. Molecular interventions 2007;7:147–156. [PubMed: 17609521]

Cummings J, Anderson L, Willmott N, Smyth JF. The molecular pharmacology of doxorubicin in vivo. Eur J Cancer 1991;27:532–535. [PubMed: 1647181]

Darley-Usmar V, Halliwell B. Blood radicals: reactive nitrogen species, reactive oxygen species, transition metal ions, and the vascular system. Pharm Res 1996;13:649–662. [PubMed: 8860419]

DeAtley SM, Aksenov MY, Aksenova MV, Carney JM, Butterfield DA. Adriamycin induces protein oxidation in erythrocyte membranes. Pharmacol Toxicol 1998;83:62–68. [PubMed: 9783322]

DeAtley SM, Aksenov MY, Aksenova MV, Harris B, Hadley R, Cole Harper P, Carney JM, Butterfield DA. Antioxidants protect against reactive oxygen species associated with adriamycin-treated cardiomyocytes. Cancer Lett 1999;136:41–46. [PubMed: 10211937]

Freeman JR, Broshek DK. Assessing cognitive dysfunction in breast cancer: what are the tools? Clin Breast Cancer 2002;3 (Suppl 3):S91–99. [PubMed: 12533269]

Gutierrez PL. The role of NAD(P)H oxidoreductase (DT-Diaphorase) in the bioactivation of quinone-containing antitumor agents: a review. Free radical biology & medicine 2000;29:263–275. [PubMed: 11035255]

Gutteridge JM. Lipid peroxidation and possible hydroxyl radical formation stimulated by the self-reduction of a doxorubicin-iron (III) complex. Biochem Pharmacol 1984;33:1725–1728. [PubMed: 6329216]

Habig WH, Pabst MJ, Jakoby WB. Glutathione S-transferases. The first enzymatic step in mercapturic acid formation. The Journal of biological chemistry 1974;249:7130–7139. [PubMed: 4436300]

Hagemann TL, Gaeta SA, Smith MA, Johnson DA, Johnson JA, Messing A. Gene expression analysis in mice with elevated glial fibrillary acidic protein and Rosenthal fibers reveals a stress response followed by glial activation and neuronal dysfunction. Human molecular genetics 2005;14:2443–2458. [PubMed: 16014634]

Handa K, Sato S. Generation of free radicals of quinone group-containing anti-cancer chemicals in NADPH-microsome system as evidenced by initiation of sulfite oxidation. Gann 1975;66:43–47. [PubMed: 239881]

Heflin LH, Meyerowitz BE, Hall P, Lichtenstein P, Johansson B, Pedersen NL, Gatz M. Cancer as a risk factor for long-term cognitive deficits and dementia. Journal of the National Cancer Institute 2005;97:854–856. [PubMed: 15928306]

Hensley K, Hall N, Subramaniam R, Cole P, Harris M, Aksenov M, Aksenova M, Gabbita SP, Wu JF, Carney JM, et al. Brain regional correspondence between Alzheimer's disease histopathology and biomarkers of protein oxidation. Journal of neurochemistry 1995;65:2146–2156. [PubMed: 7595501]

Hissin PJ, Hilf R. A fluorometric method for determination of oxidized and reduced glutathione in tissues. Analytical biochemistry 1976;74:214–226. [PubMed: 962076]

Joshi G, Hardas S, Sultana R, St Clair DK, Vore M, Butterfield DA. Glutathione elevation by gamma-glutamyl cysteine ethyl ester as a potential therapeutic strategy for preventing oxidative stress in brain mediated by in vivo administration of adriamycin: Implication for chemobrain. Journal of neuroscience research 2007;85:497–503. [PubMed: 17171703]

Joshi G, Sultana R, Tangpong J, Cole MP, St Clair DK, Vore M, Estus S, Butterfield DA. Free radical mediated oxidative stress and toxic side effects in brain induced by the anti cancer drug adriamycin: insight into chemobrain. Free Radic Res 2005;39:1147–1154. [PubMed: 16298740]

Kang SW, Chae HZ, Seo MS, Kim K, Baines IC, Rhee SG. Mammalian peroxiredoxin isoforms can reduce hydrogen peroxide generated in response to growth factors and tumor necrosis factor-alpha. The Journal of biological chemistry 1998;273:6297–6302. [PubMed: 9497357]

Kappus H. Oxidative stress in chemical toxicity. Arch Toxicol 1987;60:144–149. [PubMed: 3304204]

Konat GW, Kraszpulski M, James I, Zhang HT, Abraham J. Cognitive dysfunction induced by chronic administration of common cancer chemotherapeutics in rats. Metabolic brain disease 2008;23:325–333. [PubMed: 18690526]

Koppal T, Drake J, Butterfield DA. In vivo modulation of rodent glutathione and its role in peroxynitrite-induced neocortical synaptosomal membrane protein damage. Biochim Biophys Acta 1999;1453:407–411. [PubMed: 10101259]

Krapfenbauer K, Engidawork E, Cairns N, Fountoulakis M, Lubec G. Aberrant expression of peroxiredoxin subtypes in neurodegenerative disorders. Brain research 2003;967:152–160. [PubMed: 12650976]

Lien YC, Lin SM, Nithipongvanitch R, Oberley TD, Noel T, Zhao Q, Daosukho C, St Clair DK. Tumor necrosis factor receptor deficiency exacerbated Adriamycin-induced cardiomyocytes apoptosis: an insight into the Fas connection. Molecular cancer therapeutics 2006;5:261–269. [PubMed: 16505099]

Lu KP, Hanes SD, Hunter T. A human peptidyl-prolyl isomerase essential for regulation of mitosis. Nature 1996;380:544–547. [PubMed: 8606777]

Mark RJ, Lovell MA, Markesbery WR, Uchida K, Mattson MP. A role for 4-hydroxynonenal, an aldehydic product of lipid peroxidation, in disruption of ion homeostasis and neuronal death induced by amyloid beta-peptide. Journal of neurochemistry 1997;68:255–264. [PubMed: 8978733]

Markesbery WR, Lovell MA. Four-hydroxynonenal, a product of lipid peroxidation, is increased in the brain in Alzheimer's disease. Neurobiology of aging 1998;19:33–36. [PubMed: 9562500]

Meister A. Mitochondrial changes associated with glutathione deficiency. Biochim Biophys Acta 1995;1271:35–42. [PubMed: 7599223]

Meister A, Anderson ME. Glutathione. Annu Rev Biochem 1983;52:711–760. [PubMed: 6137189]

Meyers CA. Neurocognitive dysfunction in cancer patients. Oncology. Williston Park 2000;14:75–79. discussion 79, 81–72, 85. [PubMed: 10680150]

Morciano M, Burre J, Corvey C, Karas M, Zimmermann H, Volknandt W. Immunoisolation of two synaptic vesicle pools from synaptosomes: a proteomics analysis. Journal of neurochemistry 2005;95:1732–1745. [PubMed: 16269012]

Neumann CA, Krause DS, Carman CV, Das S, Dubey DP, Abraham JL, Bronson RT, Fujiwara Y, Orkin SH, Van Etten RA. Essential role for the peroxiredoxin Prdx1 in erythrocyte antioxidant defence and tumour suppression. Nature 2003;424:561–565. [PubMed: 12891360]

Nies AT, Jedlitschky G, Konig J, Herold-Mende C, Steiner HH, Schmitt HP, Keppler D. Expression and immunolocalization of the multidrug resistance proteins, MRP1-MRP6 (ABCC1–ABCC6), in human brain. Neuroscience 2004;129:349–360. [PubMed: 15501592]

Perluigi M, Sultana R, Cenini G, Di Domenico F, Memo M, Pierce WM, Coccia R. Redox proteomics identification of 4-hydroxynonenal-modified brain proteins in Alzheimer's disease: Role of lipid peroxidation in Alzheimer's disease pathogenesis. Proteomics - Clinical Applications 2009;3:682–693. [PubMed: 20333275]

Poon HF, Calabrese V, Calvani M, Butterfield DA. Proteomics analyses of specific protein oxidation and protein expression in aged rat brain and its modulation by L-acetylcarnitine: insights into the mechanisms of action of this proposed therapeutic agent for CNS disorders associated with oxidative stress. Antioxidants & redox signaling 2006;8:381–394. [PubMed: 16677085]

Poon HF, Vaishnav RA, Butterfield DA, Getchell ML, Getchell TV. Proteomic identification of differentially expressed proteins in the aging murine olfactory system and transcriptional analysis of the associated genes. Journal of neurochemistry 2005;94:380–392. [PubMed: 15998289]

Reed T, Perluigi M, Sultana R, Pierce WM, Klein JB, Turner DM, Coccia R, Markesbery WR, Butterfield DA. Redox proteomic identification of 4-hydroxy-2-nonenal-modified brain proteins in amnestic mild cognitive impairment: insight into the role of lipid peroxidation in the progression and pathogenesis of Alzheimer's disease. Neurobiology of disease 2008a;30:107–120. [PubMed: 18325775]

Reed TT, Pierce WM Jr, Turner DM, Markesbery WR, Butterfield DA. Proteomic identification of nitrated brain proteins in early Alzheimer's disease inferior parietal lobule. Journal of cellular and molecular medicine. 2008b

Reed TT, Pierce WM, Markesbery WR, Butterfield DA. Proteomic identification of HNE-bound proteins in early Alzheimer disease: Insights into the role of lipid peroxidation in the progression of AD. Brain research 2009;1274:66–76. [PubMed: 19374891]

Sarafian TA, Verity MA, Vinters HV, Shih CC, Shi L, Ji XD, Dong L, Shau H. Differential expression of peroxiredoxin subtypes in human brain cell types. Journal of neuroscience research 1999;56:206–212. [PubMed: 10494109]

Sayre LM, Zelasko DA, Harris PL, Perry G, Salomon RG, Smith MA. 4-Hydroxynonenal-derived advanced lipid peroxidation end products are increased in Alzheimer's disease. Journal of neurochemistry 1997;68:2092–2097. [PubMed: 9109537]

Schagen SB, Hamburger HL, Muller MJ, Boogerd W, van Dam FS. Neurophysiological evaluation of late effects of adjuvant high-dose chemotherapy on cognitive function. J Neurooncol 2001;51:159–165. [PubMed: 11386413]

Schnurra I, Bernstein HG, Riederer P, Braunewell KH. The neuronal calcium sensor protein VILIP-1 is associated with amyloid plaques and extracellular tangles in Alzheimer's disease and promotes cell death and tau phosphorylation in vitro: a link between calcium sensors and Alzheimer's disease? Neurobiology of disease 2001;8:900–909. [PubMed: 11592857]

Schulz JB, Lindenau J, Seyfried J, Dichgans J. Glutathione, oxidative stress and neurodegeneration. Eur J Biochem 2000;267:4904–4911. [PubMed: 10931172]

Sheline CT, Choi DW. Neuronal death in cultured murine cortical cells is induced by inhibition of GAPDH and triosephosphate isomerase. Neurobiology of disease 1998;5:47–54. [PubMed: 9702787]

Sies H. Glutathione and its role in cellular functions. Free radical biology & medicine 1999;27:916–921. [PubMed: 10569624]

Singal PK, Li T, Kumar D, Danelisen I, Iliskovic N. Adriamycin-induced heart failure: mechanism and modulation. Molecular and cellular biochemistry 2000;207:77–86. [PubMed: 10888230]

Smith CV, Jones DP, Guenthner TM, Lash LH, Lauterburg BH. Compartmentation of glutathione: implications for the study of toxicity and disease. Toxicology and applied pharmacology 1996;140:1–12. [PubMed: 8806864]

Stadtman ER, Berlett BS. Reactive oxygen-mediated protein oxidation in aging and disease. Chem Res Toxicol 1997;10:485–494. [PubMed: 9168245]

Sultana R, Boyd-Kimball D, Cai J, Pierce WM, Klein JB, Merchant M, Butterfield DA. Proteomics analysis of the Alzheimer's disease hippocampal proteome. J Alzheimers Dis 2007;11:153–164. [PubMed: 17522440]

Sultana R, Boyd-Kimball D, Poon HF, Cai J, Pierce WM, Klein JB, Markesbery WR, Zhou XZ, Lu KP, Butterfield DA. Oxidative modification and down-regulation of Pin1 in Alzheimer's disease hippocampus: A redox proteomics analysis. Neurobiology of aging 2006a;27:918–925. [PubMed: 15950321]

Sultana R, Boyd-Kimball D, Poon HF, Cai J, Pierce WM, Klein JB, Merchant M, Markesbery WR, Butterfield DA. Redox proteomics identification of oxidized proteins in Alzheimer's disease hippocampus and cerebellum: an approach to understand pathological and biochemical alterations in AD. Neurobiology of aging 2006b;27:1564–1576. [PubMed: 16271804]

Sultana R, Butterfield DA. Oxidatively modified GST and MRP1 in Alzheimer's disease brain: implications for accumulation of reactive lipid peroxidation products. Neurochem Res 2004;29:2215–2220. [PubMed: 15672542]

Sultana R, Poon HF, Cai J, Pierce WM, Merchant M, Klein JB, Markesbery WR, Butterfield DA. Identification of nitrated proteins in Alzheimer's disease brain using a redox proteomics approach. Neurobiology of disease 2006c;22:76–87. [PubMed: 16378731]

Takahashi K, Uchida C, Shin RW, Shimazaki K, Uchida T. Prolyl isomerase, Pin1: new findings of post-translational modifications and physiological substrates in cancer, asthma and Alzheimer's disease. Cell Mol Life Sci 2008;65:359–375. [PubMed: 17965833]

Tangpong J, Cole MP, Sultana R, Estus S, Vore M, St Clair W, Ratanachaiyavong S, St Clair DK, Butterfield DA. Adriamycin-mediated nitration of manganese superoxide dismutase in the central nervous system: insight into the mechanism of chemobrain. Journal of neurochemistry 2007;100:191–201. [PubMed: 17227439]

Tangpong J, Cole MP, Sultana R, Joshi G, Estus S, Vore M, St Clair W, Ratanachaiyavong S, St Clair DK, Butterfield DA. Adriamycin-induced, TNF-alpha-mediated central nervous system toxicity. Neurobiology of disease 2006;23:127–139. [PubMed: 16697651]

Tangpong J, Sompol P, Vore M, St Clair W, Butterfield DA, St Clair DK. Tumor necrosis factor alpha-mediated nitric oxide production enhances manganese superoxide dismutase nitration and mitochondrial dysfunction in primary neurons: an insight into the role of glial cells. Neuroscience 2008;151:622–629. [PubMed: 18160224]

Thongboonkerd V, Luengpailin J, Cao J, Pierce WM, Cai J, Klein JB, Doyle RJ. Fluoride exposure attenuates expression of Streptococcus pyogenes virulence factors. The Journal of biological chemistry 2002;277:16599–16605. [PubMed: 11867637]

Watson WH, Chen Y, Jones DP. Redox state of glutathione and thioredoxin in differentiation and apoptosis. Biofactors 2003;17:307–314. [PubMed: 12897452]

Wheeler CR, Salzman JA, Elsayed NM, Omaye ST, Korte DW Jr. Automated assays for superoxide dismutase, catalase, glutathione peroxidase, and glutathione reductase activity. Analytical biochemistry 1990;184:193–199. [PubMed: 2327564]

Winkler KE, Swenson KI, Kornbluth S, Means AR. Requirement of the prolyl isomerase Pin1 for the replication checkpoint. Science (New York, NY 2000;287:1644–1647.

Yim MB, Chae HZ, Rhee SG, Chock PB, Stadtman ER. On the protective mechanism of the thiol-specific antioxidant enzyme against the oxidative damage of biomacromolecules. The Journal of biological chemistry 1994;269:1621–1626. [PubMed: 8294408]

Zhou XZ, Lu PJ, Wulf G, Lu KP. Phosphorylation-dependent prolyl isomerization: a novel signaling regulatory mechanism. Cell Mol Life Sci 1999;56:788–806. [PubMed: 11212339]

a.

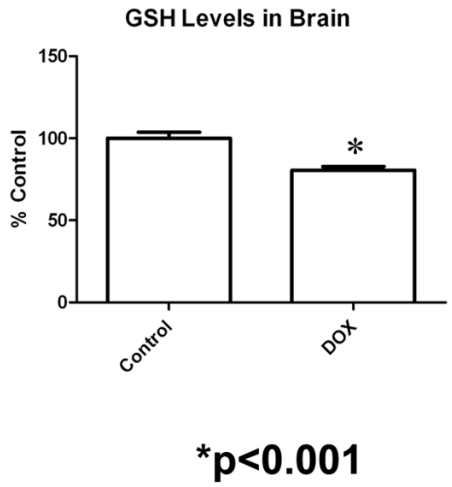


*p<0.001

b.

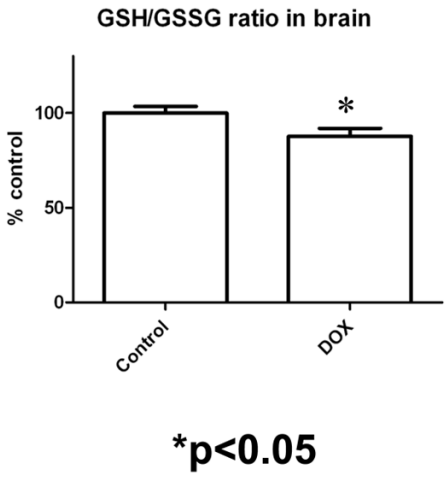


*p<0.05

**Figure 1.**

Figure 1a and b. a) Reduced GSH levels in brain isolated from saline-injected and ADR-injected mice, 72 h post i.p. injections. A significant reduction in GSH level is seen in brain isolated from ADR-injected mice when compared to control. * $p < 0.001$. b.) Decreased GSH/GSSG ratio in brain isolated from saline injected mice and ADR mice. The data are presented as mean ± SEM expressed as percentage of control. (*$p < 0.05$, n=4 controls, n=5 ADR)

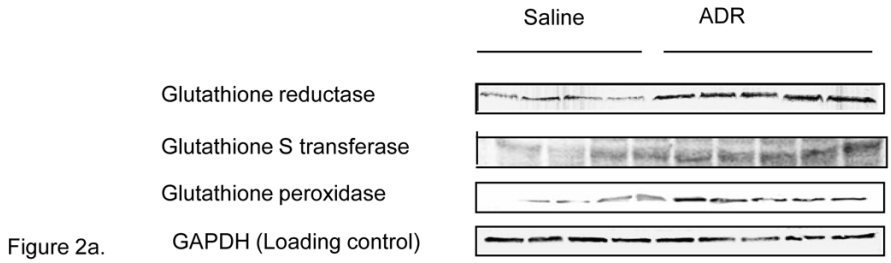


Figure 2a.

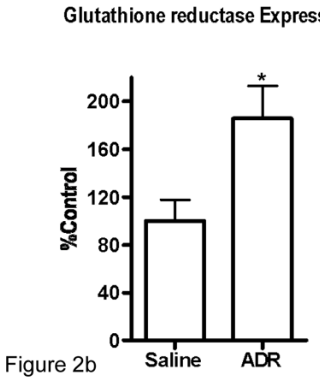


Figure 2b

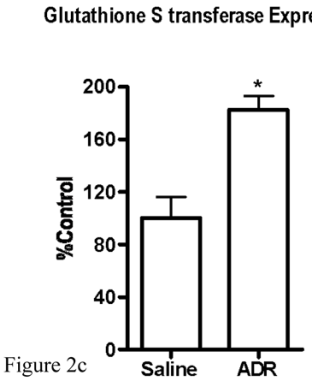


Figure 2c

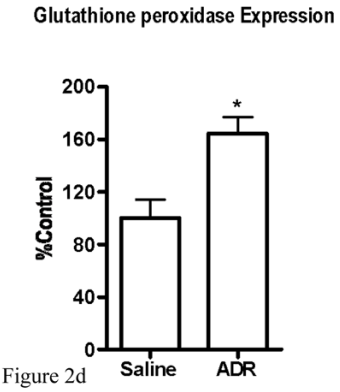


Figure 2d

**Figure 2.**

Figure 2a. Representative Western blot of brain GPx, GST, and GR 72 h post i.p. injection of saline or ADR in mice. GAPDH was used as a loading control. (n=4 controls, n=5 ADR)

Figure 2b. Representative plot of GR levels in brain isolated from saline-injected and ADR-injected mice, 72 h post i.p. injections. A significant increase in GR levels is seen in ADR-injected mice brain when compared to control. * $p < 0.05$. The data are presented as mean ± SEM expressed as percentage of control. (n=4 controls, n=5 ADR)

Figure 2c. Representative plot of GST levels in brain isolated from saline-injected and ADR-injected mice, 72 h post i.p. injections. A significant increase in GST level is seen in ADR-injected mice brain when compared to control. * $p < 0.05$. The data are presented as mean ± SEM expressed as percentage of control. (n=4 controls, n=5 ADR)

Figure 2d. Representative plot of GPx levels in brain isolated from saline-injected and ADR-injected mice, 72 h post i.p. injections. A significant increase in GST level is seen in ADR-injected mice brain when compared to control. * $p < 0.05$. The data are presented as mean ± SEM expressed as percentage of control. (n=4 controls, n=5 ADR)

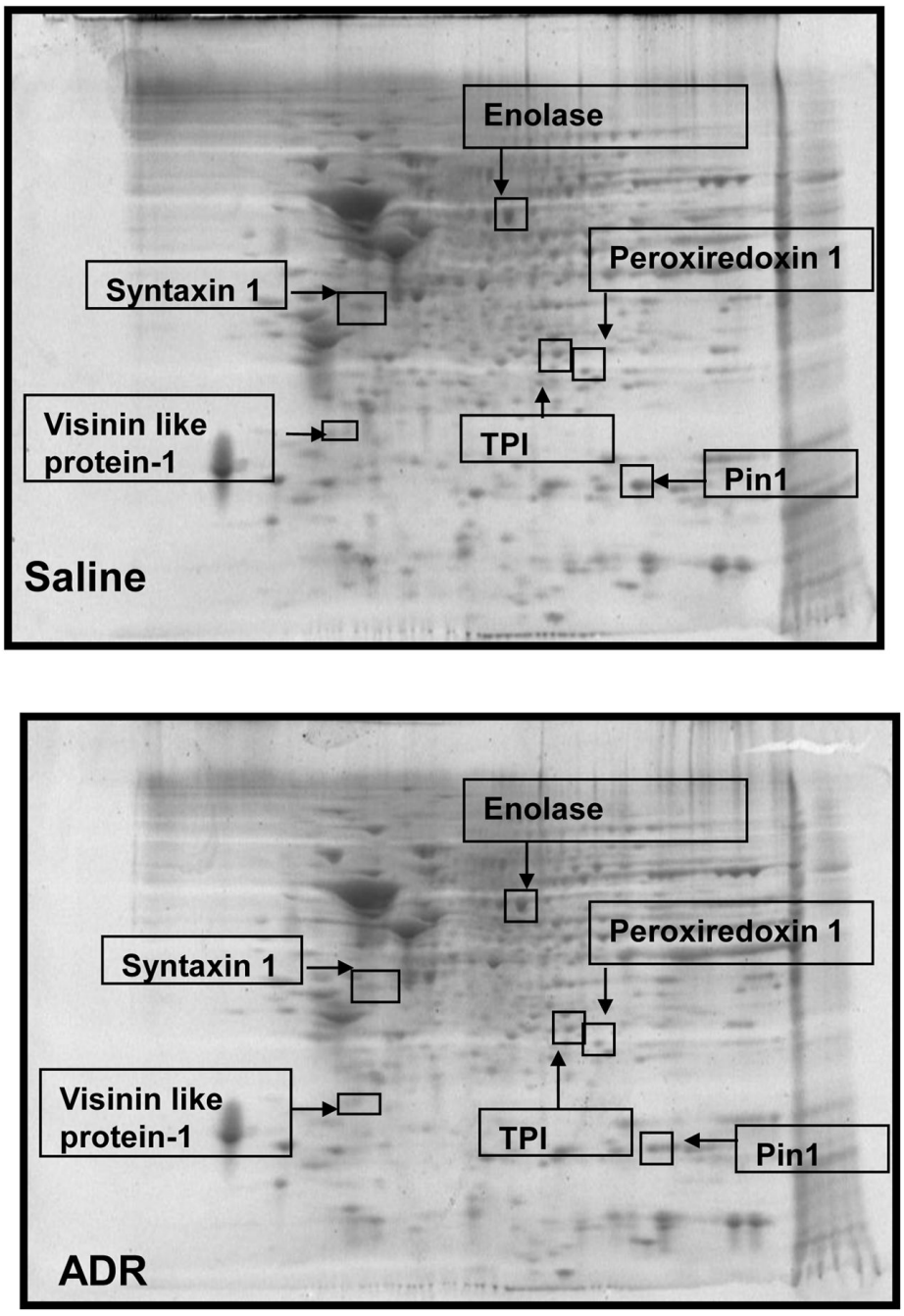


**Figure 3.**

Representative 2D gels from brains of saline- and ADR-treated mice, respectively, showing geographical location of proteins on 2D gel identified by mass spectrometry that showed differences in expression or oxidation as a result of i.p ADR. Spots that showed a significant difference in expression or oxidation levels are boxed and labeled with the corresponding protein identity. (n=4 controls, n=5 ADR)

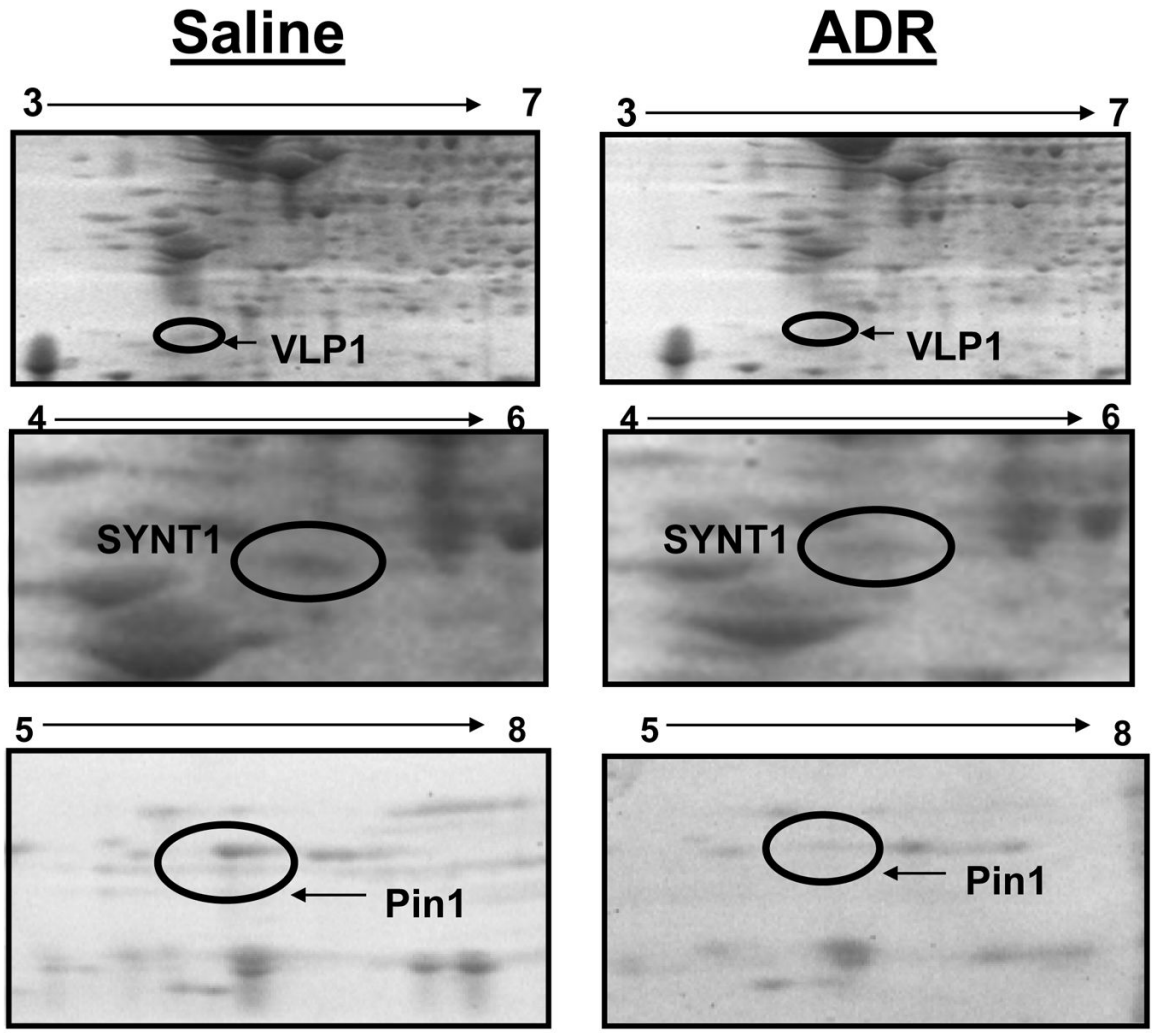


**Figure 4.**
Magnified 2D gel map areas containing spots with significant expression differences in ADR and saline-treated mice brains. All proteins identified by arrows were significantly decreased in brain with ADR treatment.

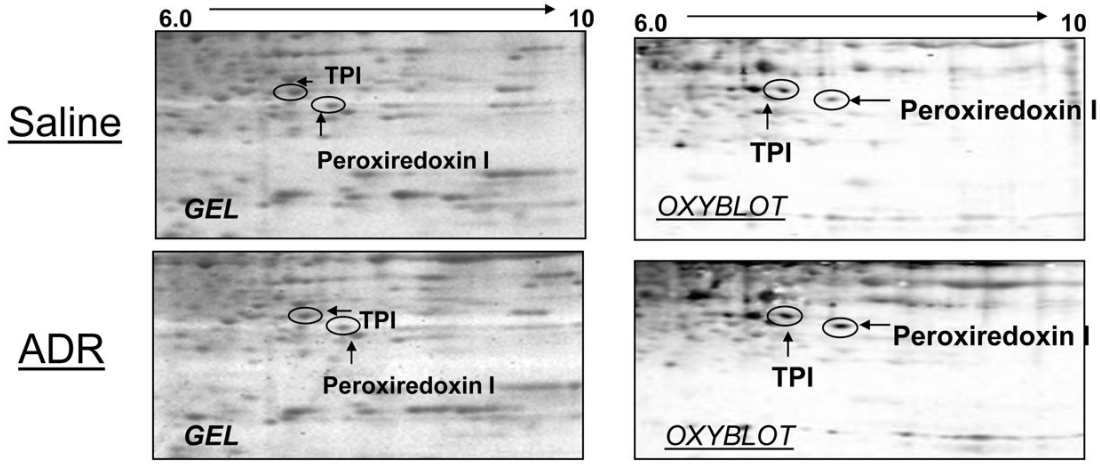


Figure 5a.

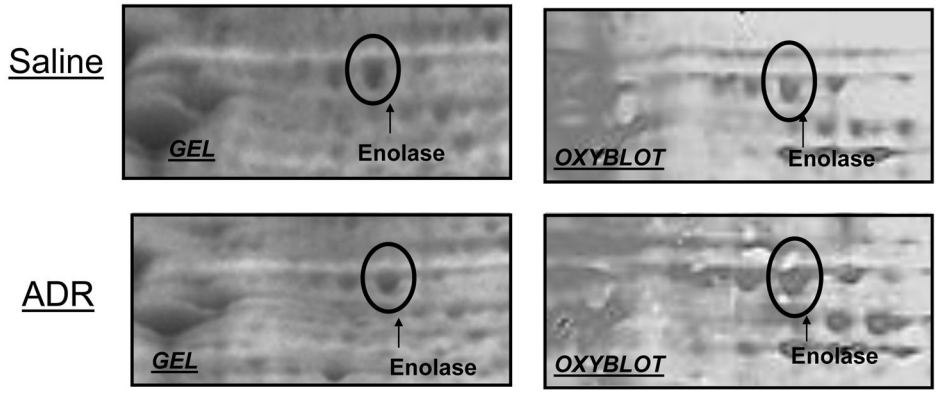


Figure 5b.

**Figure 5.**

Figure 5a & b. Magnified 2d gel and oxyblots containing significantly oxidized spots in ADR and saline-treated mice. All proteins identified showed an increase in specific oxidation in brain after i.p. administration of ADR.

## Table 1

Activities of GSH-related enzymes in brain isolated from mice treated i.p. with saline or ADR[A]

| Enzyme | Brain from saline-injected Group | Brain from ADR-injected Group |
|---|---|---|
| GST (nmol CDNB conjugate formed $min^{-1}$ $mg^{-1}$ protein) | 15.6 ± 0.34 | 12.1 ± 0.3* |
| GPx (nmol NADPH oxidized $min^{-1}$ $mg^{-1}$ protein) | 83.7 ± 0.75 | 96.9 ± 0.72* |
| GR (nmol NADPH oxidized $min^{-1}$ $mg^{-1}$ protein) | 34.9 ± 1.6 | 27.2 ± 2.3* |

[A] The data are presented as mean ± SEM (n=4,5).

* $p<0.05$.

**Table 2**

Proteins observed by proteomics as having decreased levels in brain isolated from ADR treated mice relative to control

| Protein | # of peptides matched | % Sequence coverage | MOWSE | Fold Change (ADR/Control) | P value of change | pI/MW (kDa) | Gi accession no. |
|---|---|---|---|---|---|---|---|
| Pin 1 | 6 | 41 | 68 | 0.56 | 0.029 | 7.88/18.0 | gi\|9QUR7 |
| Syntaxin1 | 8 | 36 | 145 | 0.43 | 0.026 | 5.25/33.4 | gi\|47117767 |
| Visinin like protein-1 | 9 | 45 | 107 | 0.20 | 0.039 | 5.01/22.7 | gi\|51338697 |

**Table 3**

Proteomics-determined increases in specific oxidation of proteins in brain isolated from mice treated i.p. with ADR relative to controls

| Protein | # of peptides matched | % sequence coverage | MOWSE | Fold Oxidation (ADR/Control) | P value of change | pI/MW (kDa) | Gi accession no |
|---|---|---|---|---|---|---|---|
| Peroxiredoxin1 | 9 | 45 | 134 | 4.93 | 0.041 | 8.26/22.4 | gi\|547923 |
| TPI | 8 | 39 | 77 | 6.82 | 0.046 | 7.08/26.9 | gi\|2851390 |
| Enolase | 15 | 45 | 186 | 2.30 | 0.012 | 6.36/47.0 | gi\|13637776 |